

LA-UR- 96-3962

CONF-960813J--18

Los Alamos National Laboratory is operated by the University of California for the United States Department of Energy under contract W-7405-ENG-36.

TITLE: DEVELOPMENT OF IMPLoding LINERS WITH KINETIC ENERGIES
>100 MJ AND THEIR APPLICATIONS

AUTHORS: Robert E. Reinovsky (DX-DO) and Carl A. Ekdahl (NWT-PO)

SUBMITTED TO: The Seventh International Conference on Megagauss Magnetic Field
Generation and Related Topics; August 5-10, 1996;
Sarov (Arzamas-16), Russia

DISTRIBUTION OF THIS DOCUMENT IS UNLIMITED

ph

MASTER

By acceptance of this article, the publisher recognizes that the U.S. Government retains a nonexclusive, royalty-free license to publish or reproduce the published form of this contribution, or to allow others to do so, for U.S. Government purposes.

The Los Alamos National Laboratory requests that the publisher identify this article as work performed under the auspices of the U.S. Department of Energy.

Los Alamos

Los Alamos National Laboratory
Los Alamos, New Mexico 87545

DISCLAIMER

This report was prepared as an account of work sponsored by an agency of the United States Government. Neither the United States Government nor any agency thereof, nor any of their employees, make any warranty, express or implied, or assumes any legal liability or responsibility for the accuracy, completeness, or usefulness of any information, apparatus, product, or process disclosed, or represents that its use would not infringe privately owned rights. Reference herein to any specific commercial product, process, or service by trade name, trademark, manufacturer, or otherwise does not necessarily constitute or imply its endorsement, recommendation, or favoring by the United States Government or any agency thereof. The views and opinions of authors expressed herein do not necessarily state or reflect those of the United States Government or any agency thereof.

DISCLAIMER

**Portions of this document may be illegible
in electronic image products. Images are
produced from the best available original
document.**

DEVELOPMENT OF IMPLoding LINERS WITH KINETIC ENERGIES >100 MJ AND THEIR APPLICATIONS

R. E. REINOVSKY, C. E. EKDAHL

LOS ALAMOS NATIONAL LABORATORY
LOS ALAMOS, NEW MEXICO 87545

I. Introduction:

The Los Alamos program in High Energy Density Physics is developing high performance imploding liners as sources of high energy density environments for experimental physics applications. High performance liners are, for these purposes, liners with high velocity, 100 MJ or more kinetic energy at 20-50 MJ/cm of height. They must have sufficient azimuthal symmetry, axial uniformity and density to perform as high quality impactors on central, cylindrical targets. Scientific applications of such liners are numerous and varied. For example, the properties of materials at extreme energy densities can be assessed in such an experimental environment. The physics of plasmas near solid density can be studied and hydrodynamics experiments at high Mach number (above 5?) in materials that are near solid density and significantly ionized can be conducted. In addition, liners with substantial kinetic energy and good integrity at velocities of one to a few cm/ μ sec are make good implosion drivers for fusion plasmas in the context of magnetized target fusion and MAGO.

II. High Kinetic Energy Liners

The Los Alamos program investigates the behavior of materials and of hydrodynamic system at temperatures where a substantial fraction of the material is ionized and densities approach solid. Simple estimates show that at shock pressures around 100 Mbar, single shock induced temperatures of 10-30 eV can be achieved in a variety of media at or above normal density. Well diagnosed hydrodynamics experiments demand dimensions large enough to allow the phenomenology to develop on experimental time scales and to permit good diagnostic access and resolution. Such an environment should also enable materials experiments in samples characteristic of real fabrication processes. As an example such an experiment we consider a target volume of 2 cm diameter (1 cm radius) and two centimeters high. For scoping purposes, we consider a room temperature, normal density imploding cylindrical impactor such as tungsten impacting a homogeneous cylindrical target. We can apply simple shockwave relationship:

$$P = \rho v_s u_p$$

matching the pressure, P , and the particle velocity, u_p , at the impact interface. Here ρ is the density of either the impactor or target material, and v_s is the velocity of the shock in either material. We relate the shock velocity to the particle velocity by the linear approximation

$$u_s = C + S u_p$$

which, of course, is inadequate at a phase transitions and which may be suspect at elevated energy densities. In Table 1 we present scoping values of pressure, particle velocity and shock speed in the target as a function of impactor/target material combinations and impact velocities.

From the Table we see that pressures in the range of 10-100 Mbar can be expected but that higher pressures require impactor velocities as high as 40 km/sec. Furthermore, since C and S are similar in both liner and target and, after impact, u_p is the same in both, the shock velocities are comparable in both the impactor and the target. For useful experiments the first shock in the target should at least reach the center before the rarefaction from the outside of the liner reaches the impactor/target interface.

TABLE I				
TARGET - IMPACTOR	IMPACT VELOCITY	PARTICLE VELOCITY	SHOCK SPEED	PRESSURE
	km/sec	km/sec	km/sec	Kbar
Be/W	10	7.99	16.98	2.511
Be/W	20	15.77	25.73	7.512
Be/W	30	23.52	34.44	14.994
Be/W	40	31.26	43.13	24.955
Al/W	10	7.61	15.53	3.194
Al/W	20	14.89	25.28	10.164
Al/W	30	22.12	34.97	20.882
Al/W	40	29.33	44.63	35.348
Cu/W	10	6.01	12.85	6.870
Cu/W	20	11.77	21.44	22.459
Cu/W	30	17.51	29.99	46.745
Cu/W	40	23.25	38.54	79.728
W/W	10	5.00	10.21	9.807
W/W	20	10.00	16.41	31.524
W/W	30	15.00	22.62	65.152
W/W	40	20.01	28.82	110.691

This leads to the criteria that upon impact, the liner should be at least half as thick as the target radius. Thus we can define the mass of the impactor and calculate the kinetic energy in the liner just prior to impact and we find that for a tungsten liner at 40 km/sec the kinetic energy is >60 MJ/cm in height and this sets the basic energy scale for the problem.

To further characterize the interaction, Figure 1 shows the result of a one-dimensional hydrodynamic calculation in cylindrical geometry of a 5 mm thick, room temperature tungsten impactor at 35 km/sec interacting with a 1 cm radius cylindrical aluminum target. Figure 1a shows the pressure profile as a function of radius in the target for four times after the impact. In the figure we see the shock pressure in the target approaching 100 Mbar as the shock approaches the axis. While some useful experiments can be done on the axis of the system, others can best be performed off the axis where a shock from the impact sweeps past the test location. For some applications the second shock, reflected from the axis may also be useful. Figure 1b,c,d present the pressure, temperature and density as a function of time at a point in the target material that is initially half way between the center and the target radius. This position moves with the target material (a Lagrangian zone) after the first shock and the figures plot the conditions that would be experienced by a sample placed in this "midpoint" position. Conditions for tungsten, copper and beryllium target materials are presented. Shock velocities in the low density beryllium are higher than in the tungsten target and the 5 μ s window shows the passage of the first shock and one shock reflected from the axis for tungsten. For beryllium three full cycles of converging/reflected shocks are shown as the liner continues to compress the beryllium. The temperature after the first shock ranges from 10 eV in beryllium to almost 20 eV in tungsten. Subsequent reflected shocks have only modest effect on material temperature. Densities are approximately three times normal after the passage of the first strong shock. While of only limited use, it is interesting to note that in tungsten the first reflected shock boosts the pressure at the sample station to almost a gigabar and after three cycles the pressure in beryllium exceeds half a gigabar.

To complete the scoping of the problem we can estimate the electrical energy required. Selecting a minimum liner height of 2 cm (to be comparable to the target diameter of 2 cm) implies about 120 MJ of kinetic energy and we find that electrical energies from 200-400 MJ and currents from 280 to 200 MA will be required.

Critical Issues

While high energy liners offer promise of opening significant areas of experimentation, the technological issues limiting the development and application of such liners are equally challenging. The principle issues fall into five major categories:

1. Electrical power sources capable of producing hundreds of megajoules of electrical energy at currents exceeding 150 MA will be needed.

2. While in principle enormous electrical power sources can be assembled from a large array of individual building blocks, high energy liners, unlike lasers, require that the electrical energy be delivered directly to the (liner) load as current. Thus limitations of high current transmission lines suitable for currents of hundreds of MA in practical sizes must be addressed.
3. The analysis in Section II is based on a room temperature liner arriving at the target. In practice a magnetically imploded liner will be subjected to significant ohmic heating during implosion and that heating can lead to melting, loss of material strength, reduction in liner density or even explosion (vaporization) before the liner can reach the target.
4. Assuming that the one dimensional issues can be addressed, the stability of the liner to magneto-Raleigh-Taylor effects, influenced by implosion geometry, material strength and fabrication precision may limit either the distance through which the liner can be accelerated, the magnitude of the acceleration or both, thus placing a limit on the final velocity of the liner.
5. Even if liner distortion growing in the central part of the liner can be controlled, the liner interacts with current carrying walls and that interaction may seed instability growth or result in massive disruption of the liner at the walls.

Electrical Pulse Power Sources

For electrical energies below 50 MJ, large capacitor banks have been shown to be practical and reasonably affordable energy sources. Large drivers for lasers while not delivering current to a common load have been built at or above the 50 MJ level and high performance systems at the 15-30 MJ energy level are operating or planned for the near future. Above 150 MJ however such capital intensive system may simply be unaffordable in the foreseeable future, and explosive pulse power with its combination of high performance and low capital cost represents an attractive option.

To date the Disk Explosive Magnetic Generator¹, a flux compressor configuration developed and tested at VNIIEF has been demonstrated to be viable candidate for large currents and energies. Russian and US calculational models, Russian experiments and joint Russian/US diagnostics have lead to a working understanding of these configurations². Using models that have been calibrated against experimental data for DEMG systems of both 40 and 100 cm diameter, we can characterize the performance of such generators as a function of the load inductance. Figure 2 shows the performance of a conceptual 100 cm diameter DEMG initially loaded to 6.6 MA and operated into a fixed inductance load. The calculation includes elementary hydrodynamic estimates of wall motion including magnetic pressure to describe the geometric change in the inductance of the flux compression cavity; current diffusion and non-linear heating of the walls and flux loss due to non-linear magnetic diffusion into the walls. While diffusion losses in the load inductance are not explicitly calculated, losses in transmission lines coupling cavities to the load are included. Figure 2a shows the peak current, current gain and flux conservation calculated as a function of load inductance per module. For small load (<0.25nh/module) more than half the flux is lost in diffusion and heating losses and peak currents are limited to 450 MA or less. For larger loads, only 5% of the flux is lost to the conductors and peak current is limited by flux conservation. Figure 2b shows the energy delivered as a function of load inductance per module and energy delivery peaks at 25 MJ/module and about 0.25nh/module. For the DEMG configurations individual models are connected in series increasing the load inductance that can be driven in direct proportion to the number of cavities.

The DEMG is a coaxial system with the liner load connected at one end and initial flux introduced into the other. Conceptually, this limits diagnostics of the experiment to those that can be applied to one side of the load and this can represent a significant disadvantage. The Rancho system is also a modular system that is being developed at Los Alamos to provide two sided access to an implosion load. As shown in Figure 3, Rancho is a parallel connected array of simultaneously initiated coaxial flux compressors delivering current on parallel transmission plates to a central load. Since modules are connected in parallel, the current deliverable by the system increases with the number of modules as shown reaching about 350 MA for a four module system. However, the parallel connection means that the gain of the system decreases as modules are added.

Transmission Lines for Current Delivery

While pulse power generators conceptually capable of producing the currents and energies needed to drive high energy liners are available now and new ones may be demonstrated in the near future, current delivery systems capable of delivering hundreds of megamps to liners represent a significant challenge. Coaxial systems such as the DEMG can, in principle be designed to match the liner's initial radius so that only a modest length of coaxial transmission line is required to connect the liner to the generator. On the other hand a common design of sufficiently large radius coupled to the liner with a section of parallel plate line where current converges radially may be the most cost effective design approach for the future. A modular system such as Ranchero clearly requires the equivalent of a radial section delivering current to the liner. Finally, every liner system requires that current densities approaching 10 MA/cm must be delivered at the final stages of an implosion for a liner is designed to drive a 1 cm radius target. Thus current densities of 1 MA/cm must be considered and if even higher current density transmission lines can be designed, flexibility will be improved.

To characterize the behavior of a transmission line at high current density, the results of a 1-D MHD calculation are presented in Figure 4. For the calculation a current waveform typical of a DEMG driving a liner load was employed. The transmission line conductors was characterized by a 2 mm conducting layer of copper and an inertial/structural layer of steel, 20 mm thick. The coaxial line has a radius of 500 mm (1 meter diameter). The rise-time of the current was about 50 μ s and the implosion time about 20 μ s. The amplitude of the driving current was scaled by a simple factor to provide peak currents of 180, 360 and 720 MA. The calculation addressed conductor motion, magnetic diffusion and non-linear conductor heating. It included an elementary strength model following Steinberg for both the copper and steel layers. The calculations tracks the flux transported past the initial position of the conductor as a function of time and from the ratio of flux transport to current, a time dependent inductance change in the transmission line was determined. Figure 4 shows the results of the calculation expressed as nH/m for circumferential current densities of 0.5, 1.0 and 2.0 MA/cm. Noting that implosion of the liner occurs about 70 μ s, after the start of the DEMG, the figure shows that at current densities less than 1MA/cm the increase in transmission line inductance is significantly less than 1 nH in a meter long line while for current densities of 2 MA.cm the inductance increase rapidly rises to an almost unacceptable 3-4 nH/m. This suggests that for transmission lines of any significant length, current densities up to or perhaps modestly exceeding 1 MA/cm can be applied. Current densities above about 1.5 MA/cm will likely be unacceptable in conventional transmission lines.

One Dimensional Implosion Dynamics

To characterize the one dimensional behavior of liners, it is useful to consider the analytically simplest implosion system, that of a inductor in which energy is stored by virtue of an initial current. The inductor is directly connected to an imploding liner as shown in Figure 5a. By conceptually treating the circuit elements as perfect conductors and the liner as a perfectly conducting, the circuit equations reduce to a statement of flux conservation within the store and the volume swept out by the liner during its motion (ΔL). From flux conservation, the kinetic energy in the liner can be immediately written in terms of ΔL , :

$$KE = \Delta L / (L_s + \Delta L) \times \frac{1}{2} L_s I_0^2 = \frac{1}{2} M V_T^2$$

where M is the mass of the liner and V_T is the velocity at the time the line arrives at the target. With this model it is straight forward to calculate the liner velocity at the time of collision with a target of fixed radius (1 cm.). Figure 5b shows parameters of the liner at collision in parameter space of velocity and kinetic energy per centimeter length for a fixed initial energy in L_s of 100 MJ. The inductance of the storage inductor ranges from 1 to 50 nH and the currents range from 450 MA to 63 MA respectively. Target radii are limited for practical reasons to lie between 10 and 50 cm. And liner heights from 1 to 10 cm are considered.. The figure shows one representative point (R=20, h=2, M=100 gr, L_s =5nH) which delivers about 35 MJ of kinetic energy at 36 km/sec to a 1 cm target. Curves through the point represent the trajectory through energy/velocity space that results from varying one geometric parameter: radius, height or mass – for a fixed pulse power driver (L_s , I_0) – while holding other geometric parameters

constant. The changing mass trajectory is a horizontal line in energy/velocity space because kinetic energy determined by flux conservation is independent of mass. Hence impact velocity varies simply as $\sqrt{2E/M}$. Velocity can, in principle be increased without limit by decreasing the mass of the liner, and this is of course, the logic that leads to z pinch plasma implosions for producing high temperature plasmas. For liners used as shock producing impactors however, a limiting criteria on liner performance is that most of the mass of the liner should arrive at the target at near normal density. This imposes a minimum limitation on the mass (and a maximum limitation on the velocity) of the liner. For the plot, we impose the limit that the average action in the liner not exceed vaporization specific action ($A < 5 \times 10^{16}$). Dotted portions of the curves show where average action exceeds the vaporization limit

Variations in height clearly have the large impact on energy with only modest impact on velocity. Increasing height increases total kinetic energy coupled to the liner in the flux conserving approximation. But since total energy is limited, increasing liner height decreases kinetic energy per unit height of the liner. From this we conclude that the shortest liner that is otherwise practical provides the best performance. In the flux conserving approximation, variations with radius are seen to have least impact on liner performance when both mass and height are held constant.

The representative point discussed above has the property that the mass, radius and height trajectories all transition to average action in excess of the vaporization limit at this point. The representative point is thus a local optimum point for the specific pulse power system (L_s, I_0) selected. A similar local optimization can be performed for other combinations of L_s and I_0 . Holding the height constant at 2 cm a minimum value chosen to provide an approximately cubic experimental volume with a 2 cm diameter target), the heavy curves on the plot show the locus of points limited by vaporization average action for radii of 10 and 50 cm. The heavy curves show that in general smaller diameter implosions lead to higher velocities. Further more, maximum velocities can be achieved at storage inductances around 5 nH but velocities above 40 km/sec can be achieved for storage inductances ranging from 2-18 nH.

While not shown here, similar characterizations performed for higher stored energies show that storage inductance between 2.5-10nH remain optimum and kinetic energy per unit length increase approximately with the stored energy.

The flux conservation model provides a general outline of parametric variations based on average specific action. In a real liner -- and especially in one in which the implosion starts with maximum current in the inductive store -- current and magnetic field are initially limited to the outside of the liner and penetrate into the liner as the implosion proceeds. One dimensional MHD calculations such as those displayed in Figure 6 characterize the condition of the liner just before impact with a 1 cm target. The calculation is performed for roughly the parameters of the representative point in Figure 5. The liner has initial radius of 20 cm, mass of 78 gr/cm and initial thickness of 2.3 mm and has been accelerated to an inner surface velocity of 32.6 Km/sec and 35 MJ/cm upon impact. The plot shows the density, temperature, pressure and velocity as a function of radius just before impact on the target. The plot shows that at this time the inner 2 mm of the liner is below the ambient melt temperature for aluminum (933 K) while the inner 4 mm is below ambient vaporization temperature. On the other hand peak density is almost 5 gr/cc and the inner 16 mm (almost 95 % of liner mass) is above normal density. In general the liner displayed in Figure 6 represents a good impactor for experiments at velocities up to 33 km/sec.

However, substantially higher velocities are required to produce pressures of interest. For example to produce a shock pressure above 40 Mbar in a medium density target (copper) an aluminum liner must reach a velocity above 49 km/sec but a 200 MJ of stored energy is required to drive the 88 gr liner!. Calculations similar to those shown in Figure 6 show that while such velocities can be reached with a homogeneous aluminum liner, the temperature of the entire liner is above 1eV. Simple Hugoniot considerations show that if the liner were tungsten, the required impact velocity would be only 27 km/sec, and the liner mass can be almost 133 grams. Unfortunately the relatively poor conductivity of a tungsten liner leads to excessive ohmic heating during implosion. A compromise approach is that of a composite system made of a tungsten impactor surrounded by an aluminum current carrying liner. Figure 7 shows the results of a calculation for such a liner consisting of 102 gram of aluminum and a 131 gram tungsten impactor. The calculation shows that the peak density in the tungsten is 29 gr/cc and the tungsten remains virtually at room temperature, suggesting that composite liners can provide useful impactors.

Two Dimensional Stability

The one dimensional calculations presented above suggest that straight-forward application of existing technology can provide imploding liners with the material density, velocity and kinetic energy needed to produce useful high energy environments. Experiment require, in addition, that the impactor arrive with sufficient azimuthal symmetry and axial uniformity to produce nearly one dimensional shocks in the target. Magnetically imploded cylindrical liners are subject to fluid instabilities on their outer surface when the magnetic pressure produces stress in the liner that exceeds the yield strength. For liners of radius of 20 cm and thickness of 1-4 mm currents of 1.5-3 MA are sufficient to exceed the yield stress in the liner. First principles analytic theory shows that while instabilities will to grow, strength effects in the liner will reduce the instability growth rate and may allow for satisfactory performance for some combinations of drive time and geometry. While strength effects are complicated, the case in which the entire liner is melted can be taken as the limit when strength effects can no longer inhibit instability growth. Figure 6-7 show that for an appropriate choice of geometry and drive, liners can be designed in which the inner surface and some fraction of the liner are solid retaining some strength. In fact the pressure in the line is well above ambient and since elevated pressure raises the melt temperature and using ambient melt is a conservative estimate.

To explore the development of instabilities in high energy liners, simple experiments have been conducted on the Pegasus four-megajoule capacitor bank. High purity (1100 series) aluminum liners, initially 2.4 cm in outer diameter with 0.4mm walls were imploded with currents that range from 4.3 to 6.3 MA. For these experiments the liner was initially 2 cm tall and implodes on glide planes that converge at 8° from each side. Liner behavior was assessed using medium energy radiographic imaging. To enhance the opacity and "mark" the inner surface, the liner was coated on the inside with a thin layer, less than 20μ of gold. One dimensional calculations indicated that, for a peak drive current of 4.3 MA, this standard liner, could be driven to inner surface velocities of about 4.2 km/sec, and inner surface convergence of about 4, before the inner surface reaches ambient melt temperature. At 6.3 MA the liner could be driven to higher velocities, 6.5 km/sec at convergence of 4, but full melting of the liner would be expected after the liner had converged only a factor of 1.5, and the inner surface was moving at about 3 km/sec. Examination of the radiographs for a liner driven with 4.2 MA current shows that when the liner has moved to approximately 0.75 cm radius, it is reasonably straight (axially uniform) with little evidence of instability on the outer surface and no evidence of perturbations on the inner surface the peak. At higher currents 6.3 MA, it is calculationally melted at the time at which it was radiographed at 1.6 cm radius, and shows evidence of 0.1 cm wavelength instability growing on the back surface. In addition the radiograph may show some evidence of instability perturbing the inner surface. The lower current implosion was radiographed at a radial convergence of 6 (0.4 cm radius), at this radius, the radiographs also shows evidence of large scale bending of the inner surface with the parts of the liner nearest the electrodes converging more than the parts of the liner at the midplane. Preliminary 2D calculations predict the development of distortions qualitatively similar to those seen in the radiograph. While these large scale disruptions bear qualitative resemblance to a buckling resulting from axial compression of the liner by the converging electrodes, substantial analysis is required to confirm that assessment..

SUMMARY

High Energy Liners represent a promising approach to producing high energy density environments. They are conceptually capable of producing plasmas at near solid density, tens of eV temperature, and pressures above 100 Mbar. The pulse power systems needed to drive such systems are available today and new systems both in the laboratory and in the field are under development. Power transport at current densities above 1 MA/cm will be essential to further progress in this area. In one dimension, the required liner energy, density and velocity can be achieved. Furthermore, appropriate choices of geometry and drive can produce liners with significant fractions of the mass unmelted. Composite liners offer promise of driving high density impactors to interesting velocities. Instabilities, both free surface and wall related, currently represent the major technical issue and appropriate application of strength effects are under investigation to control instability growth. Other mechanisms such a imposed axial magnetic fields and multiple shells can also be considered.

REFERENCES

1. Chernyshev, B.E. Grinevich, V.V. Vakrushev, V.I. Mamyshev, "Scaling Image of 90 MJ Explosive Magnetic Generators" // in *Megagauss Fields and Pulsed Power Systems* (ed. VM Titov and GA Shvetsov), Nova Science, 1990, pp 347-350.
2. Buyko, N.P. Bidylo, V.K. Chernyshev, V.A. Demidov, S.F. Garanin, V.N. Kostyukov, A.A. Kulagin, A.I., Kuzyaev, A.B. Mezhevov, V.N. Mokhov, E.S. Pavlovskiy, A.A. Petrukhin, V.B. Yakubov, B.T. Yegorychev, JW. Canada, C.A. Ekdahl, J.H. Goforth, J.C. King, I.R. Lindemuth, R.E. Reinovsky, P. Rodriguez, R.C. Smith, L.R. Veaser, S.M. Younger, "Results of Russian/US High-Performance DEMG Experiment", Proceedings of the Tenth IEEE International Pulsed Power Conference, Albuquerque, NM, June 1995.

FIGURE CAPTIONS

Figure 1: A cold tungsten line 0.5 cm thick, imploding at 35 km/sec impacts a 1 cm radius target producing a dense ionized plasma in the target. Radial pressure profiles (Fig 1a) and temporal pressure, temperature, density and the midpoint of the target (Fig 1b).

Figure 2: Conceptual performance of 100 cm diameter DEMG as function of load inductance calculated with a model that has been bench-marked against both 40 cm diameter and 100 cm diameter experiments.

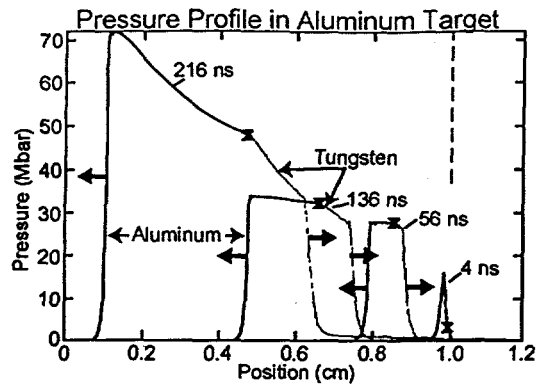
Figure 3. Configuration of a modular Rancho system consisting of parallel connected coaxial generators and conceptual performance for one to four parallel modules.

Figure 4. Motion of a 1m diameter transmission at three current densities.

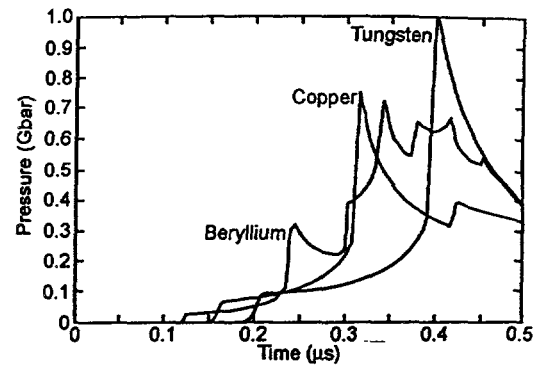
Figure 5 Simple inductive store driving an imploding liner

Figure 6 ID-MHD of liner implosion

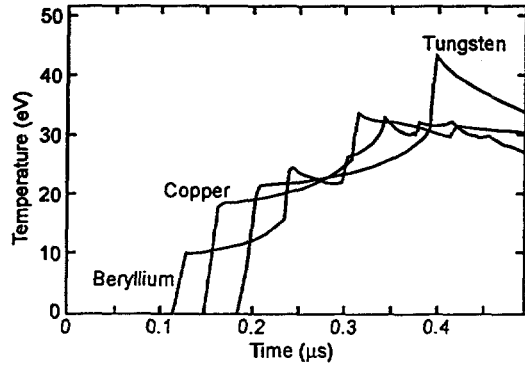
Figure 7 1D-MHD of composite liner



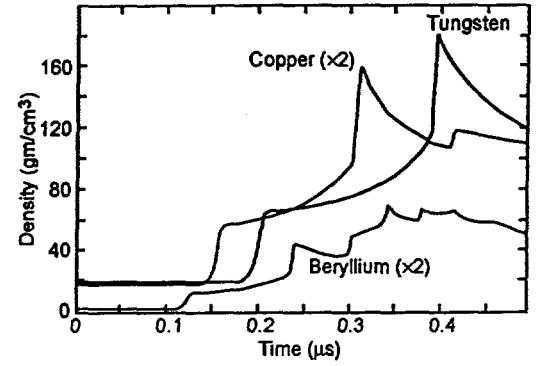
(a)



(b)

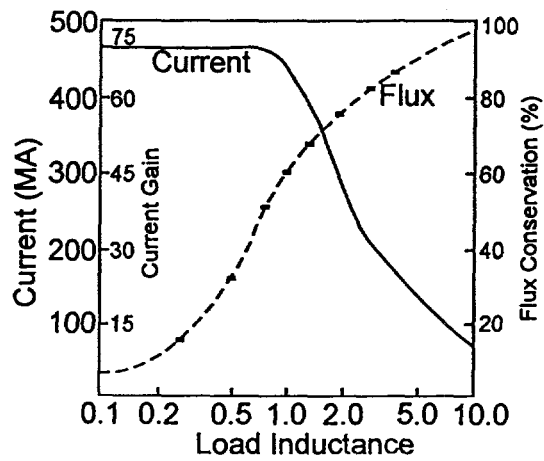


(c)

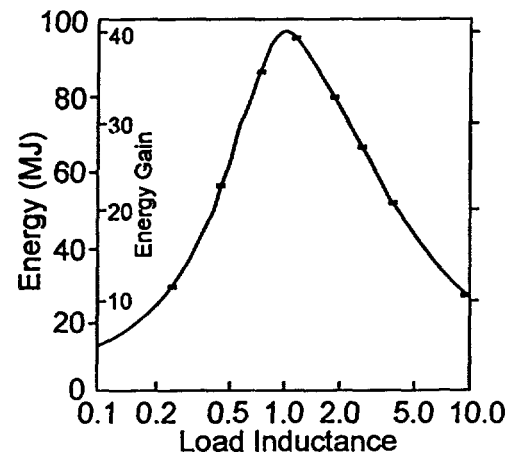


(d)

Fig. 1



(a)



(b)

Fig. 2

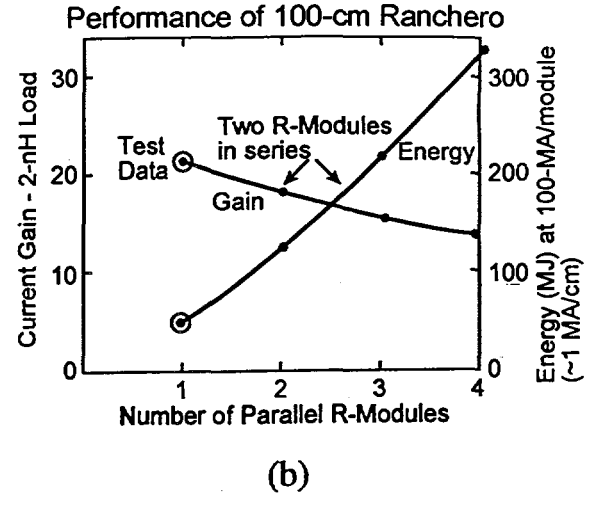
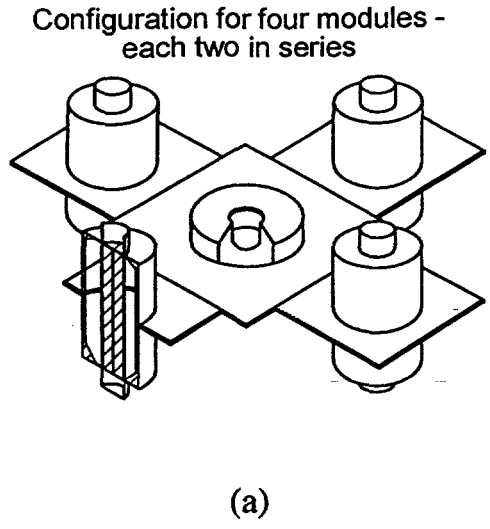


Fig. 3

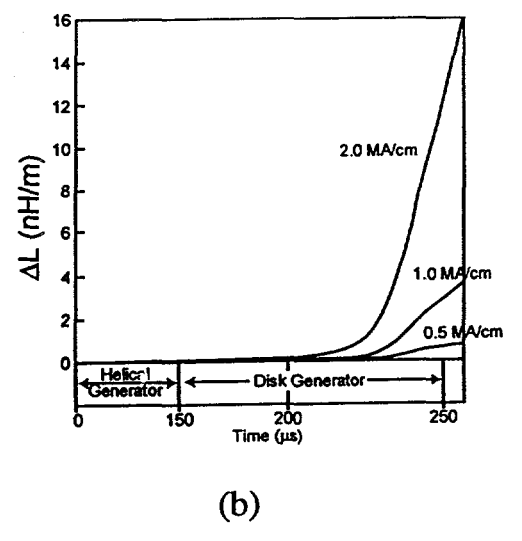
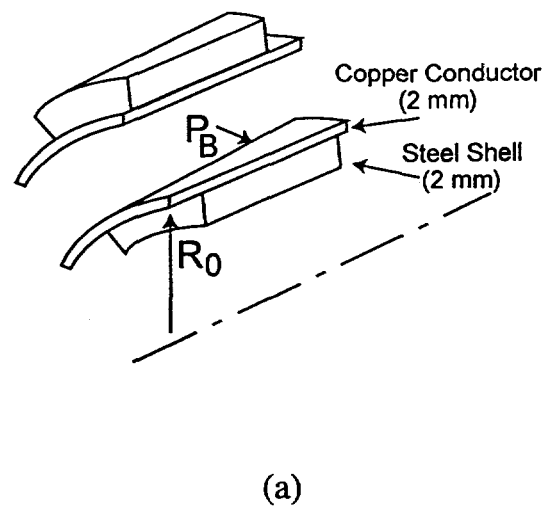
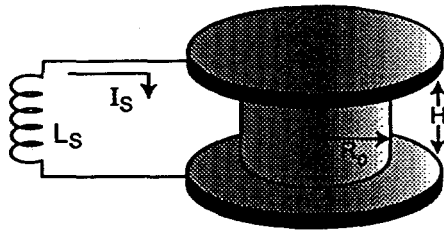
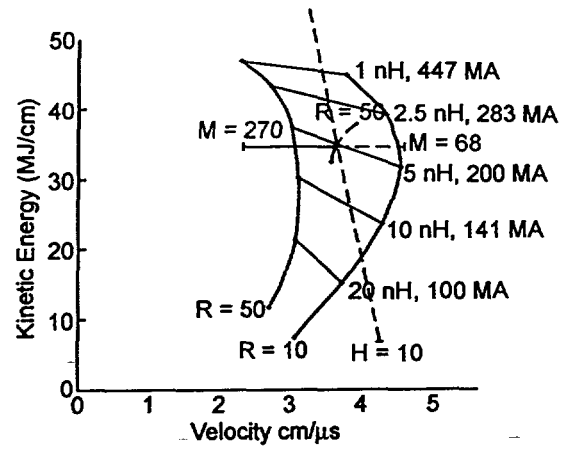


Fig. 4

Simple Inductive Store Driver-Liner



(a)



(b)

Fig. 5

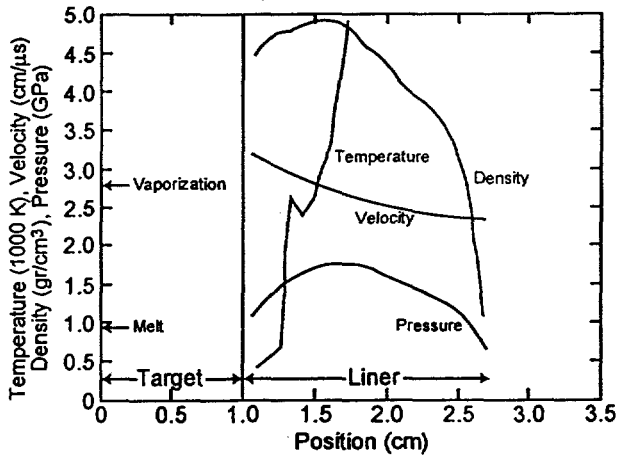


Fig. 6

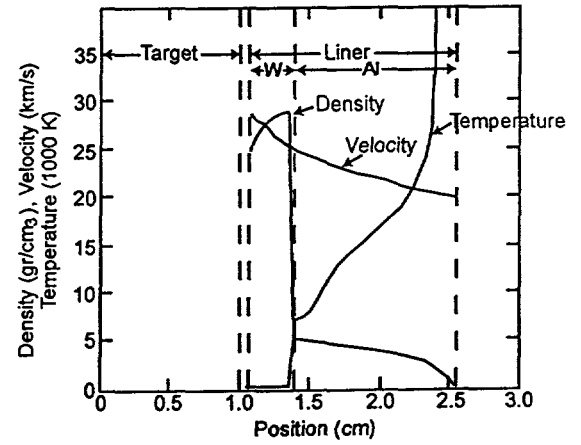


Fig. 7